Communication: Slow proton-charge diffusion in nanoconfined water

Tibert H. van der Loop,[1] Niklas Ottosson,[2] Thomas Vad,[3] Wiebke F. C. Sager,[4,a)] Huib J. Bakker,[2,b)] and Sander Woutersen[1,c)]
[1]*Van 't Hoff Institute for Molecular Sciences (HIMS), University of Amsterdam, Science Park 904, 1098 XH Amsterdam, The Netherlands*
[2]*FOM Institute for Atomic and Molecular Physics, Science Park 104, 1098 XG Amsterdam, The Netherlands*
[3]*Institut für Textiltechnik, RWTH Aachen University, Otto-Blumenthal-Strasse 1, 52074 Aachen, Germany*
[4]*Peter Grünberg Institute, Forschungszentrum Jülich GmbH, 52425 Jülich, Germany*

(Received 9 February 2017; accepted 23 March 2017; published online 7 April 2017)

We investigate proton-charge mobility in nanoscopic water droplets with tuneable size. We find that the diffusion of confined proton charges causes a dielectric relaxation process with a maximum-loss frequency determined by the diffusion constant. In volumes less than ~5 nm in diameter, proton-charge diffusion slows down significantly with decreasing size: for diameters <1 nm, the diffusion constant is about 100 times smaller than in bulk water. The low mobility probably results from the more rigid hydrogen-bond network of nanoconfined water, since proton-charge mobility in water relies on collective hydrogen-bond rearrangements. *Published by AIP Publishing.* [http://dx.doi.org/10.1063/1.4979714]

The transport of protons through nanometer-sized volumes of liquid water occurs in systems ranging from porous minerals,[1] fuel-cell membranes,[2–4] metal-organic frameworks[5–7] and zeolites,[8] to the living cell. In contrast to proton diffusion in bulk water which has been studied extensively,[9–13] comparatively little is known about proton transfer in such nanoscopic volumes. Previous work has demonstrated that the kinetics of photo-induced deprotonation and subsequent geminate recombination of photoacids can change upon nanoscopic confinement in reverse micelles.[14,15] It was however also found[15] that in reverse micelles with neutral surfactants, the photoacid molecules tend to attach to the surface (where no photo-induced deprotonation occurs), which complicates the results, while in nanoscopic reverse micelles, with ionic surfactants, the counter-ion concentration is prohibitively large: typically >10M for water-pool diameters d < 5 nm. In addition, for small reverse micelles, the size of the photoacid probe molecule becomes comparable to the water volume, which sets an intrinsic limitation to this approach. Nanoconfined proton mobility has also been investigated using quasi-elastic neutron scattering[16–19] and nuclear magnetic resonance spectroscopy.[20,21] Both these techniques, however, probe the mobility of the proton mass rather than that of the proton charge, and these mobilities can be very different due to the contribution of the Grotthuss mechanism to the proton-charge mobility.[22–24] Here, we probe the mobility of aqueous proton charges in nano-confinement directly by observing their response to an externally applied oscillating electric field. To investigate proton-charge transport in confinement, we prepare nanoscopic water volumes in self-assembling reverse micelles in cyclohexane (see supplementary material). We use a nonionic surfactant (Igepal CO-520) to avoid interfacial charge effects[25–27] and size-dependent surfactant counter-ion concentrations. Igepal contains hydroxy and ether O atoms, which have pK_b ~ 16 and 18, so protons do not "stick" to the surfactant.

Since reverse micelles can take up water molecules in their hydrophilic interior, the ratio w_0 = [H_2O]/[surfactant] can be used to tune the size of the enclosed water volumes.[28,29] We use small-angle x-ray scattering to characterize the structure of the reverse micelles.[30,31] The investigated reverse micelles have a spherical shape, a polydispersity parameter <0.2, and interact as hard spheres. We observe a linear size dependence on w_0, with a proportionality factor of 0.42 ± 0.01 nm for the water pool diameter (Fig. 1(a)). To study ions in nanoconfined water, we use appropriate aqueous solutions in the preparation of the reverse micelles. Using 1M HCl or LiCl as the interior aqueous phase has no influence on the shape or size of the reverse micelles (Fig. 1(b)).

Figures 1(c) and 1(d) show the dielectric response of spherical Igepal reverse micelles with a water-pool diameter of 4.2 nm containing neat water and 1M aqueous solutions of HCl, LiCl, NaCl, and KCl. The dielectric response arises primarily from the translational motion of ions and the reorientation of molecular dipole moments.[33] The response of the reverse micelles containing neat water (blue points) is the sum of core-water reorientation (20 GHz) and reorientation of water close to the surfactant headgroup (~0.1 GHz).[34,35] The reverse micelles containing 1M HCl (red points) exhibit an additional strong response at ~300 MHz, which is absent in the reverse micelles containing neat water. This response is also absent or much weaker for reverse micelles containing alkali chloride solutions of the same concentration,[49] and can therefore be assigned to the protons. We isolate the proton response by subtracting the response of reverse micelles prepared with neat

a)Electronic address: w.sager@fz-juelich.de
b)Electronic address: h.bakker@amolf.nl
c)Electronic address: s.woutersen@uva.nl

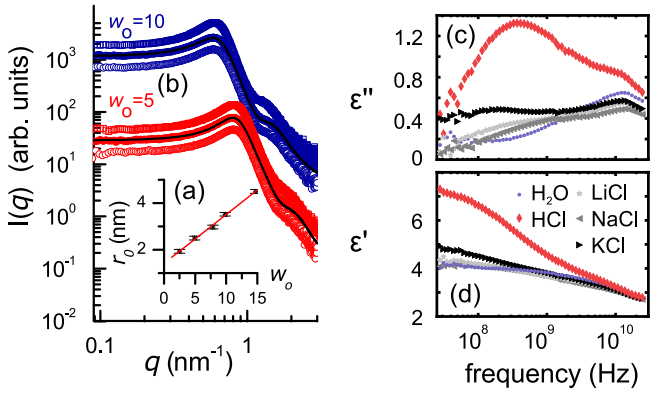

FIG. 1. (a) Linear dependence of the radius r_0 of the reverse micelle (water plus the hydrophilic head group) on w_0. Linear regression (red line) yields a proportionality factor of 0.42(1) nm between w_0 and the water-pool diameter. (b) Small-angle x-ray scattering intensity for w_0 = 5 (water-pool diameter 2.1 nm, red points) and 10 (water-pool diameter 4.2 nm, blue points). The different aqueous phases of the reverse micelles are shown as filled circles (neat water), open circles (1M HCl), and open squares (1M LiCl). The individual scattering curves are vertically displaced for better comparison. The black solid lines are least-squares fits to the water data. The shape of the curves is typical for spherical scatterers at concentrations high enough to clearly visualize the structure-factor peak. The scattering data are fitted with a multi-component model for hard spheres (see supplementary material).[32] The polydispersity parameter σ_0 is <0.2 for all investigated samples. Addition of salt does not result in significant structural changes. ((c) and (d)) Imaginary and real parts of the dielectric response of w_0 = 10 reverse micelles containing neat water (blue), 1M aqueous HCl (red), LiCl (light-grey), NaCl (grey), and KCl (black).

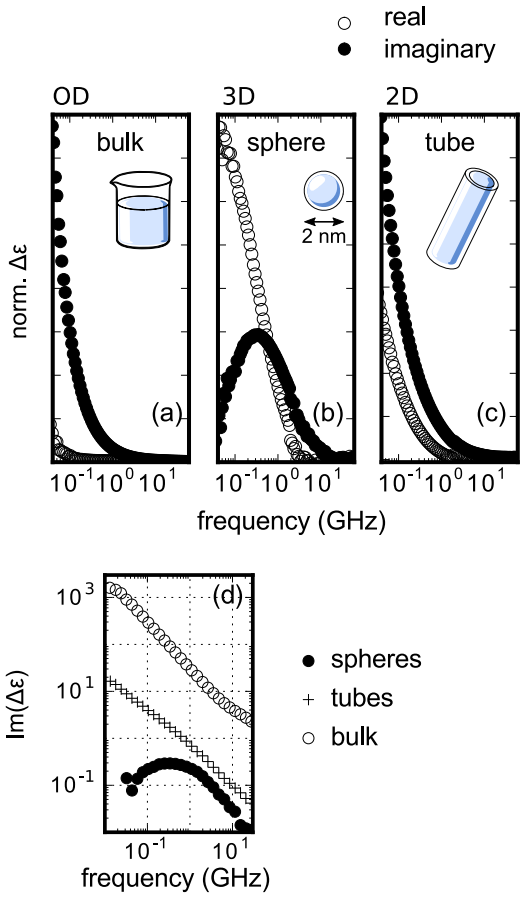

FIG. 2. Dielectric response of protons in bulk water (a) and in spherical (b) and tubular (c) confinement, both with w_0 = 5. A log-log plot of the data (d) shows the ω^{-1} response of the protons in bulk and in tubular confinement. In each case, the proton-charge response is obtained by subtracting the dielectric response in absence of HCl from that in the presence of HCl (1M solution).

water from that of reverse micelles prepared with an aqueous HCl solution. In Figures 2(a) and 2(b) we compare this proton response with that of protons in bulk water. Whereas the proton response in bulk water is purely imaginary and given by $i\kappa/\omega$ (with ω the frequency and κ the DC conductivity),[33] the protons confined in the nanodroplets exhibit the signature of a dielectric relaxation process, which occurs for all investigated droplet sizes (Fig. 3). This dielectric relaxation arises because the migration of proton charges in response to the applied electric field comes to a halt as they reach the wall of the nanodroplet; the amount of dissipated energy is maximal when the applied electric field changes sign at the moment this halting occurs (an interfacial polarization effect).[36] The maximum-loss frequency of the relaxation process is thus determined by the time scale on which the proton-charge migration comes to a halt, and hence by the size of the water droplet and the proton-charge diffusion constant. The amplitude of the dielectric response associated with the proton diffusion increases with the confinement size because in larger nanodroplets a larger polarization has been built up at the moment the proton charges reach the confining wall. The diffusion of the counter ions should cause a similar relaxation at much lower frequencies (due to the much lower diffusion constant).

To confirm that the observed relaxation process is caused by the confinement of the protons, we measure the dielectric response of protons confined in long interconnected tubular reverse micelles, prepared with the same surfactant and $[H_2O]/[surfactant]$ ratio, but using *n*-hexane instead of cyclohexane as the apolar phase. Using hexane as the apolar phase results in less efficient solvation of the hydrophobic surfactant tails, so that the interfacial surfactant layer becomes less curved towards water, causing the spherical reverse micelles to transform into interconnected tubular structures.[28,29,32,37–39] Note that due to the volume and surface area constraints, the tubular radius cannot be smaller than 2/3 of the sphere radius.[32] In these interconnected tubular reverse micelles, the proton charges do not come to a halt, and thus no relaxation process is observed (Fig. 2(c)). The absence of the relaxation process in tubular micelles (which have the same surfactant and w_0 as the spherical micelles) also excludes the possibility that the relaxation process is due to surface water. The observed dielectric response of the confined proton charges can be well described by a Cole-Cole relaxation process[40]

$$\Delta\varepsilon_{H^+}(\omega) = \frac{\Delta\varepsilon^0_{H^+}}{1-(i\omega\tau_R)^{1-\alpha}}, \quad (1)$$

where ω is the angular frequency, and $\Delta\varepsilon^0_{H^+}$, τ_R, and α are the size-dependent amplitude, relaxation time, and broadening parameter, respectively. From least-squares fits, we determine the relaxation times for all investigated droplet sizes, see Figure 3. The relaxation time (the inverse of the maximum-loss frequency) is determined by the size of the nanodroplet and the diffusion constant. Their relation can be derived from the field-induced time-dependent spatial distribution of diffusing ions confined in a spherical volume, for which we obtain an analytic expression (see supplementary material). As an example, we

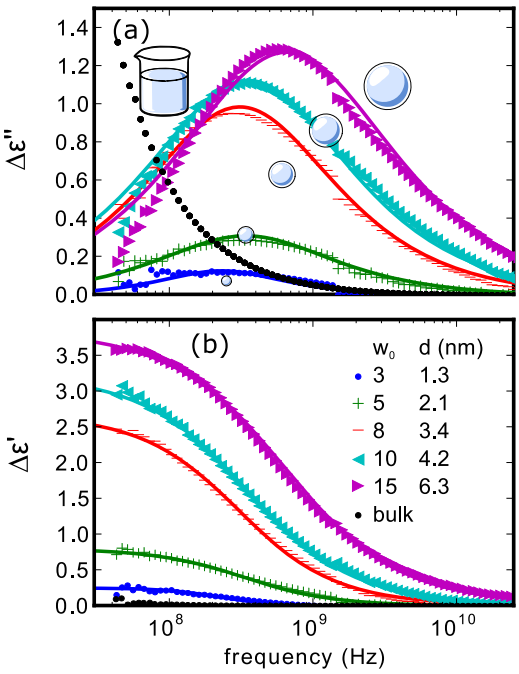

FIG. 3. Imaginary (a) and real (b) parts of the dielectric difference spectra $\Delta\varepsilon_{H^+} = \varepsilon_{HCl(aq)} - \varepsilon_{H_2O}$ showing the response of protons confined in spherical reverse micelles with different water-pool diameters. Upon increasing the reverse-micelle size, both the intensity and the center frequency increase. The black dots represent the water-background corrected response of 1M HCl solution (vertically scaled for better comparison). The curves are least-squares fits of Eq. (1) to the data.

show in Figure 4, the calculated time dependent proton distribution upon switching on a DC electric field at $t = 0$ (using a proton diffusion constant equal to the bulk value). The resulting time-dependent polarization can be Fourier transformed to obtain the dielectric response function.[41] From this analysis (see supplementary material), we find that the diffusing ions exhibit a Debye-type dielectric response with a relaxation

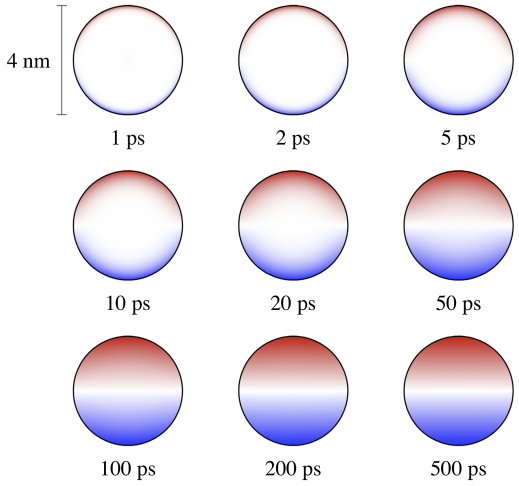

FIG. 4. Calculated time-dependent change in proton-charge distribution in a water sphere of 4 nm diameter, after switching on a DC electric field (directed vertically upward) at $t = 0$. In this calculation, we use a diffusion constant equal to the bulk value ($D = 9.3 \times 10^{-9}$ m^{2}s^{-1}). We show a cross section through the center of the sphere at increasing times. Red denotes an increase with respect to a uniform distribution, and blue a decrease. The color scale has been normalized at each time point (see supplementary material).

time

$$\tau_R = \frac{(d/2)^2}{4.33D}, \tag{2}$$

where d is the diameter of the water sphere and D the diffusion constant. Using Eq. (2) and the observed water-pool diameters and relaxation times, we determine the proton diffusion constant D_{H^+} in the nanodroplets. It should be noted that the experimentally observed proton spectra are Cole-Cole (broadened Debye) modes, whereas the theory predicts a normal Debye response ($\alpha = 0$). This broadening of the Debye mode is caused by the polydispersity of the reverse-micelle size (~10%) and by the inhomogeneity of the water structure inside the reverse micelles that gives rise to a distribution of diffusion constants, an effect that has been characterized recently using molecular dynamics simulations of water confined in surfactant phases.[42] The D_{H^+} obtained from our data is averaged over the micelle size distribution and over potential spatial inhomogeneities of the diffusion constant. We find that for small sizes (up to about 3 nm diameter), the amplitude of the dielectric response grows approximately quadratically with the nanopool size as predicted by our theoretical analysis (see supplementary material). For larger sizes, the amplitude grows less than quadratically, probably due to local-field effects[36] (the water volume fraction in the samples with large nanopool size is much larger, see supplementary material). An important advantage of our experiment is that the diffusing proton charges are observed directly and in a non-perturbative manner (the strength of the applied oscillating electric field is negligible compared to the local electric fields of molecular partial charges), and no probe molecules are required. In the remainder, we focus on the effective diffusion constant obtained by analyzing our data using Eqs. (1) and (2). A more detailed quantitative interpretation of our experiments would require state-of-the-art *ab initio* molecular-dynamics simulations, and we hope our results will stimulate work in this direction.

We find that the proton-charge diffusion constant depends strongly on the size of the nanoscopic water volume (see Fig. 5, where we have also indicated the bulk diffusion constant). For the smallest investigated water-pool diameter (1.2 nm), the diffusion constant is about 100 times smaller than in bulk water. For large droplet sizes, the proton-charge diffusion constant

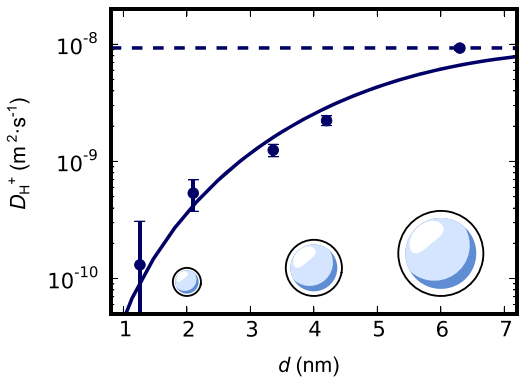

FIG. 5. Proton-charge diffusion constant in nanodroplets as a function of the water-pool diameter. The spheres above the x-axis indicate the relative sizes. The dashed line indicates the bulk proton-charge diffusion constant, and the solid line is a guide to the eye. The error bars represent 2σ.

converges to the bulk value, as expected. The slow diffusion of proton charges in the reverse micelles might partly involve binding of the protons to the surface. Previous work has shown that proton-charge diffusion along a lipid-membrane surface can be significantly slower than in bulk water.[43,44] However, in our reverse micelles the surfactant has a much lower proton-binding affinity than water (see above), so that the protons are mostly located within the water nanopool. The dielectric response of Fig. 2(b) indicates that the proton-charge diffusion slows down in the entire water nanodroplet, since if charge diffusion would be slow only in the surface layer and not in the core, we would observe different relaxation modes, corresponding to proton diffusion in the interfacial layers and proton diffusion in the core of the nanodroplet. Instead, we observe for each nanodroplet size a single relaxation mode, of which the frequency of the maximum response gradually changes with the size of the nanodroplet. Hence, the decreased proton diffusion constant appears to be a quite uniform property of the water nanodroplet. This uniform behavior presents an interesting contrast to the reorientation and hydrogen-bond dynamics of water molecules in water nanodroplets: previous work has shown evidence that in reverse micelles only a single layer of water molecules is immobilized by binding to the surfactant head groups, and that the slowing down of the hydrogen-bond dynamics is caused mostly by surface-induced restructuring of the water hydrogen-bond network.[45–47] However, proton-charge diffusion is known to involve the concerted motion of many water molecules,[22–24] and hence is intimately connected with the hydrogen-bond dynamics of a large volume of water molecules. In nanoconfined water, this concerted motion will probably also involve water molecules in the interfacial layers. The slowing down of these interfacial water molecules contributes to the observed uniform slowing down of the proton-charge diffusion. However, it cannot be the main cause since even for the smallest nanopools (where proton-charge diffusion virtually comes to a standstill), the fraction of surface water is comparatively small. For instance, we found previously that in the d = 2.1 nm nanopools the surface-water fraction is slightly below 50%,[46] whereas the proton-charge diffusion is about 20 times slower than in bulk water (Figure 5). It therefore seems that a slowing down of collective water dynamics upon nanoconfinement is the main cause of the slow proton-charge diffusion in nanoconfined water. The precise confinement volume below which such collective dynamics, and thus proton-charge diffusion, slows down may be system dependent, and may be slightly larger in systems in which (unlike reverse micelles) more than one water monolayer is immobilized by surface binding.[48]

In view of the above-discussed relation between proton-charge diffusion and water dynamics, it is interesting to investigate whether a correlation exists between the average reorientation rate of the water molecules in the nanodroplets and the diffusion constant of the proton. We indeed find (Fig. S6 of the supplementary material) that the average water reorientation rate decreases in a similar manner with decreasing water volume as the proton-charge diffusion constant. However, while the diffusion constant decreases by a factor of ~100 (compared to the bulk value) for the smallest reverse micelles, the average reorientation rate of the water molecules inside these micelles is reduced by a factor of only 4. This difference can be explained from the more collective nature of the reorganization of the hydrogen-bond network required for proton-charge diffusion as compared to the rearrangement involved in the reorientation of a water molecule. The hopping of a proton charge in bulk water involves the collective reorganization of a relatively large water structure of approximately 15 water molecules.[24] The reorganization of the hydrogen-bond network required for reorientation is more local, leading to strongly different reorientation rates near the surface and in the core of the water nanodroplet. Due to this strong spatial variation of the reorientation rate over the nanodroplet, the effect of nanoconfinement on the average reorientation rate will be small compared to the effect on the proton-charge mobility.

To conclude, we report on the observation of a relaxation process in the dielectric spectrum of acidic water nanodroplets. The frequency dependence of this relaxation process provides unique information on the proton-charge mobility in nanoconfined water. The observed large influence of spherical nanoconfinement on proton-charge mobility in water should be relevant for many research fields, although it should be pointed out that care should be taken when applying our conclusions, which were obtained using spherical nanoconfinement, to protons confined in cylindrical or planar water volumes. In these geometries, a similar slowing down of the charge diffusion may be expected upon strong confinement, although the quantitative aspects might be different. In this respect it is interesting to note that the nanochannels in mesoporous materials and fuel-cell membranes typically have diameters ranging from 1 to 10 nm,[2] i.e., in the range where we here have shown that proton-charge diffusion is governed by confinement.

See supplementary material for the experimental details, our model for the dielectric response of ions diffusing in a sphere, and additional results.

This work is part of the research program of the Stichting voor Fundamenteel Onderzoek der Materie (FOM), financially supported by the Nederlandse organisatie voor Wetenschappelijk Onderzoek (NWO). The authors would like to thank H. Schoenmaker and H. J. Boluijt for technical support as well as Johannes Hunger for valuable discussions and Emmanuel Kentzinger (PGI-4, Forschungszentrum Jülich) for his help in performing the SAXS experiments. N.O. gratefully acknowledges the European Commission (FP7) for funding through the award of a Marie Curie Fellowship. S.W. acknowledges financial support from the John van Geuns Foundation.

[1] D. Muñoz-Santiburcio, C. Wittekindt, and D. Marx, Nat. Commun. **4**, 2349 (2013).
[2] K. Schmidt-Rohr and Q. Chen, Nat. Mater. **7**, 75 (2008).
[3] K.-D. Kreuer and G. Portale, Adv. Funct. Mater. **23**, 5390 (2013).
[4] J. Savage and G. A. Voth, J. Phys. Chem. Lett. **118**, 17436 (2014).
[5] G. K. H. Shimizu, J. M. Taylor, and S. Kim, Science **341**, 354 (2013).
[6] J. M. Taylor, R. K. Mah, I. L. Moudrakovski, C. I. Ratcliffe, R. Vaidhyanathan, and G. K. H. Shimizu, J. Am. Chem. Soc. **132**, 14055 (2010).
[7] F. Paesani, J. Phys. Chem. C **117**, 19508 (2013).
[8] J. Sauer, *Proton Transfer in Zeolites* (Wiley-VCH, 2007), pp. 685–707.
[9] J. T. Hynes, Nature **397**, 565 (1999).
[10] O. F. Mohammed, D. Pines, J. Dreyer, E. Pines, and E. T. J. Nibbering, Science **310**, 83 (2005).

[11]S. Woutersen and H. Bakker, Phys. Rev. Lett. **96**, 138305 (2006).
[12]J. T. Hynes, Nature **446**, 270 (2007).
[13]M. Thämer, L. D. Marco, K. Ramasesha, A. Mandal, and A. Tokmakoff, Science **350**, 78 (2015).
[14]D. B. Spry, A. Goun, K. Glusac, D. E. Moilanen, and M. D. Fayer, J. Am. Chem. Soc. **129**, 8122 (2007).
[15]C. Lawler and M. D. Fayer, J. Phys. Chem. B **119**, 6024 (2015).
[16]J.-C. Perrin, S. Lyonnard, and F. Volino, J. Phys. Chem. C **111**, 3393 (2007).
[17]S. Lyonnard, Q. Berrod, B.-A. Brüning, G. Gebel, A. Guillermo, H. Ftouni, J. Ollivier, and B. Frick, Eur. Phys. J.: Spec. Top. **189**, 205 (2010).
[18]M. L. Hoarfrost, M. S. Tyagi, R. A. Segalman, and J. A. Reimer, Macromolecules **45**, 3112 (2012).
[19]Q. Berrod, S. Lyonnard, A. Guillermo, J. Ollivier, B. Frick, and G. Gébel, EPJ Web Conf. **83**, 02002 (2015).
[20]Q. Berrod, S. Lyonnard, A. Guillermo, J. Ollivier, B. Frick, A. Manseri, B. Améduri, and G. Gébel, Macromolecules **48**, 6166 (2015).
[21]J. Hinterberg, A. Adams, B. Blümich, P. Heitjans, S. Kim, Z. A. Munir, and M. Martin, Phys. Chem. Chem. Phys. **15**, 19825 (2013).
[22]M. E. Tuckerman, D. Marx, M. L. Klein, and M. Parrinello, Science **275**, 817 (1997).
[23]D. Marx, M. E. Tuckerman, J. Hutter, and M. Parrinello, Nature **397**, 601 (1999).
[24]K. J. Tielrooij, R. L. A. Timmer, H. J. Bakker, and M. Bonn, Phys. Rev. Lett. **102**, 198303 (2009).
[25]M. Kondo, I. A. Heisler, J. Conyard, J. P. H. Rivett, and S. R. Meech, J. Phys. Chem. B **113**, 1632 (2009).
[26]B. Guchhait, R. Biswas, and P. K. Ghorai, J. Phys. Chem. B **117**, 3345 (2013).
[27]A. A. Bakulin, D. Cringus, P. A. Pieniazek, J. L. Skinner, T. L. C. Jansen, and M. S. Pshenichnikov, J. Phys. Chem. B **117**, 15545 (2013).
[28]*Micelles, Membranes, Microemulsions, and Monolayers*, edited by W. M. Gelbart, A. Ben-Shaul, and D. Roux (Springer, New York, 1994).
[29]W. F. C. Sager, in *Nanostructured Soft Matter, Experiment, Theory, Simulation and Perspectives*, edited by A. V. Zvelindovsky (Springer, Dordrecht, 2007), pp. 3–44.
[30]A. Vrij and C. G. de Kruif, in *Micellar Solutions and Microemulsions, Structure, Dynamics, and Statistical Thermodynamics*, edited by S. H. Chen and R. Rajagopalan (Springer, New York, 1990), pp. 143–155.
[31]T. Zemb, in *Neutrons, X-Rays and Light Scattering Methods Applied to Soft Condensed Matter*, edited by P. Lindner and T. Zemb (Elsevier, North-Holland, Amsterdam, 2002), pp. 317–350.
[32]T. H. van der Loop, N. Ottosson, S. Lotze, E. Kentzinger, T. Vad, W. F. C. Sager, H. J. Bakker, and S. Woutersen, J. Chem. Phys. **141**, 18C535 (2014).
[33]J. Barthel, R. Buchner, K. Bachhuber, H. Hetzenauer, M. Kleebauer, and H. Ortmaier, Pure Appl. Chem. **62**, 2287 (1990).
[34]R. Biswas, N. Rohman, T. Pradhan, and R. Buchner, J. Phys. Chem. B **112**, 9379 (2008).
[35]W. Wachter, G. Trimmel, R. Buchner, and O. Glatter, Soft Matter **7**, 1409 (2011).
[36]K. Asami, Prog. Polym. Sci. **27**, 1617 (2002).
[37]M. Kahlweit, R. Strey, D. Haase, H. Kunieda, T. Schmeling, B. Faulhaber, M. Borkovec, H. F. Eicke, G. Busse, F. Eggers *et al.*, J. Colloid Interface Sci. **118**, 436 (1987).
[38]S. A. Safran, *Statistical Thermodynamics of Surfaces, Interfaces, and Membranes* (Addison-Wesley, Reading, 1994).
[39]E. M. Blokhuis and W. F. C. Sager, J. Chem. Phys. **115**, 1073 (2001).
[40]C. J. F. Böttcher and P. Bordewijk, *Theory of Electric Polarization* (Elsevier, Amsterdam, 1978), Vol. 2.
[41]R. Kubo, M. Toda, and N. Hashitsume, *Statistical Physics II, Nonequilibrium Statistical Mechanics* (Springer, Berlin, 1985).
[42]S. Hanot, S. Lyonnard, and S. Mossa, Nanoscale **8**, 3314 (2016).
[43]T. Yamashita and G. A. Voth, J. Phys. Chem. B **114**, 592 (2010).
[44]L. Xu, L. N. Öjemyr, J. Bergstrand, P. Brzezinski, and J. Widengren, Biophys. J. **110**, 1993 (2016).
[45]D. E. Moilanen, N. E. Levinger, D. B. Spry, and M. D. Fayer, J. Am. Chem. Soc. **129**, 14311 (2007).
[46]T. H. van der Loop, M. R. Panman, S. Lotze, J. Zhang, T. Vad, H. J. Bakker, W. F. C. Sager, and S. Woutersen, J. Chem. Phys. **137**, 044503 (2012).
[47]A. Schlaich, E. W. Knapp, and R. R. Netz, Phys. Rev. Lett. **117**, 048001 (2016).
[48]S. Gruener, T. Hofmann, D. Wallacher, A. V. Kityk, and P. Huber, Phys. Rev. E **79**, 067301 (2009).
[49]We tentatively assign the weak feature around 0.1 GHz in the alkali solutions to the diffusion of the alkali ions.